Int J Mech Mater Des (2009) 5:353–364
DOI 10.1007/s10999-009-9107-5

Analysis of predicted residual stress in a weld and comparison with experimental data using regression model

Mahyar Asadi · John A. Goldak · Jason Nielsen · Jianguo Zhou · Stainslav Tchernov · Daniel Downey

Received: 6 October 2009 / Accepted: 19 October 2009 / Published online: 2 November 2009

Abstract Residual stress in a welded plate is computed in the first part of the paper using a weld analysis software program VrWeld (www.goldaktec.com) that computes the 3D transient temperature field, the evolution of micro-structure and the evolution of stress-strain fields. The computed residual stress is compared to the residual stress distribution measured by Paradowska (J Mater Process 164–165: 1099–1105, 2005) with a neutron diffraction method to show that the computational model captures the physics well. Two uncertainty analyses are conducted in the second part to investigate the question of how variations in parameters contribute to the result from part one provided that computational model can predict residual stress well resulted in part one. The difference between the two is the number of parameters. The former has only one parameter and we employed the computational model for perturbation analysis in order to find the uncertainty due to perturbation in the parameter. For such a test, the number of test required in sample space to approximate normality by central limit theorem, is feasible considering computational resources although it is not true when we have higher number of interrelated parameters. The latter therefore has 4 highly interrelated parameters to show that an alternative way can be employed instead of using directly computational model for such a case. Uncertainty analyses are based on Monte Carlo method in this paper and the idea is that if numerical modeling is valid and also there is a need for a great number of tests for Monte Carlo analysis that make it unfeasible to run such an analysis directly by computational model then extracting a regression model from the computational model and working with it, is an effective alternative.

Keywords Residual stress · Numerical modeling · Weld · Experimental data · Regression model

M. Asadi (✉) · J. A. Goldak
Department of Mechanical and Aerospace Engineering, Carleton University, Ottawa, ON, Canada
e-mail: masadi@connect.carleton.ca

J. A. Goldak
e-mail: jgoldak@mrco2.carleton.ca; johngoldak@goldaktec.com

J. Nielsen
Department of Mathematics and Statistics, Carleton University, Ottawa, ON, Canada
e-mail: jdn@math.carleton.ca

J. Zhou · S. Tchernov · D. Downey
Goldak Technologies Inc., Ottawa, ON, Canada

1 Introduction

Manufacturing processes generate residual stresses in the structure before in-service loading is applied. This changes the in-service behavior of structure. The considerable residual stress that welding adds to a welded structures is a concern for designers. Residual

stresses are caused by incompatible internal strains and they vary over the life cycle of a structure. They often contribute to early fatigue failure. The residual stresses are usually not known to design engineers in many cases and this lack of knowledge leads to conservative design practices that are expected to increase costs and reduce the performance of welded structures. This motivated Paradowska et al. (2005) to embark on a research program to measure residual stresses in welds.

Residual stresses can be measured by neutron/X-ray diffraction based on Bragg's reflection equation or other methods. However it is expensive to accurately measure residual stresses. The high cost of such measurements further limits the use of experimental measurements by designers to control and mitigate the effect of residual stresses. The measurements are inherently discrete and often limited to tens of points. This small set of data points is a coarse sampling of a full 3D field of the residual stress in a welded structure.

Prediction of residual stresses by numerical modeling is a desirable complement to experimentally measured residual stresses. Although recent numerical modeling is a powerful tool for predicting residual stress, validation with a reference to experimental results is essential to have confidence in the model and the algorithm.[1]

Designer's would like to mitigate the undesirable effects of residual stresses in as-welded structures by an appropriate selection of material, welding process and parameters, structural geometry and fabrication sequence. This can be done best if the designer has a reliable predictive model that can be used in the early design stages. In this sense, validation is a measure of the extent that the design model and the real design agree and the extent that they differ.

Validation is not complete unless it considers the variation induced by uncertainties in parameter values. For example, material properties or process parameters for numerical modeling often are seen as a fixed value in computation although they are not fixed value in reality and they are estimation involving inevitable inherent variation. Does this variation result in a significant change in the response? This is the question the designer needs to know a priori.

2 Experimental data

Paradowska et al. (2005) has recently presented a set of experimental data of residual stress measured by neutron diffraction. The residual stress was measured at room temperature in the unrestrained specimen after the plate cooled to room temperature.

Their experimental set up for the weld is shown in Fig. 1. The specimen is a low-carbon steel plate $100 \times 200 \times 12$ mm. The filler metal is 14 mm wide and 6 mm high. The composition of the plate and filler metal are given in Table 1. The flux-cored arc welding process used a 1.6 mm diameter electrode with a 20 mm contact tip to work distance. ARGOSHIELD 52 shielding gas was used with a gas flow rate of 18 l/min. The welding parameters were 260–280 amps, 28–30 volts and a welding speed of 6 mm/s. During welding the specimen rested on a plate but was free to move with no constraints other than rigid body motion.

3 Numerical algorithm

A three-dimensional model and meshes were created to accurately model the 3D experimental set up described in Sect. 2. The mesh had 3,628 8-node brick and 166 6-node prism elements and 5,724 nodes. The computing time on a single core of a

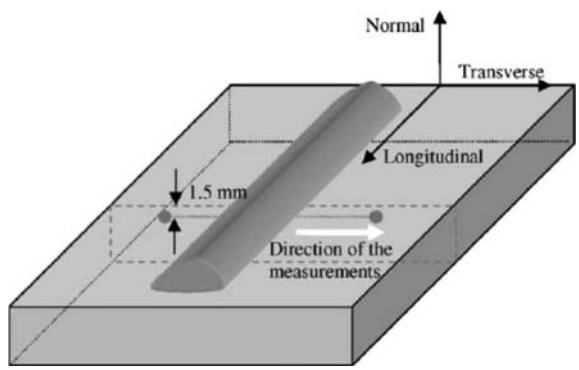

Fig. 1 Experimental setup that shows the filler metal on the $200 \times 100 \times 12$ mm plate and the line along which the elastic strain profile is measured

[1] ASME V &V 10-2006, Guide for Verification and Validation in Computational Solid Mechanics, An American National Standard, The American Society of Mechanical Engineers.

Table 1 Chemical composition of parent and consumable materials (in wt%)

Composition	C	Mn	Si	S	P	Ni	Cr	Mo	Cu	V	Ti	Co	Al
Parent metal	0.12	0.63	0.13	0.01	0.01	0.02	0.02	0.01	0.01	<0.01	<0.01	<0.01	0.03
Weld metal	0.10	1.76	0.68	0.02	0.02	0.05	0.03	0.04	–	0.04	–	–	–

2.66 GHz Intel Core 2 quad computer was 39 s for thermal analysis, 18 s for microstructure analysis and 12.2 min for stress analysis.

3.1 Thermal analysis

The thermal analysis of the weld used a double ellipsoid model to capture the heating effect of the welding arc (Goldak et al. 1984). The dimensions of the double ellipsoid shown in Fig. 2 were width $b = 7$ mm, height $c = 6$ mm, front length $a_2 = 7$ mm and trailing length $a_1 = 4$ mm. The transient analysis used 51 time steps including a cool-down period with exponentially increasing time step sizes.

The thermal properties were taken from Anderson (1978). The transient energy equation was solved with a convection boundary condition with a temperature dependent convection coefficient $h(T) = 5.0 + 0.05(T - 300) + 6 \times 10^{-7}\,(T - 300)^3$ (w/m^2 K) for $300 < T < 1700$°K (Kumar et al. 2008).

Figure 3 illustrates the snapshots of the transient temperature fields at times 3.5 and 25 s.

3.2 Microstructure analysis

The microstructure evolution follows the algorithms described in Watt et al. (1988) and Henwood et al. (1988). These algorithms extend the theory in Kirkaldy and Venugoplan (1983). The essential idea is that a pseudo-Iron-Carbon phase diagram in which all lines and points are functions of the alloy composition is used to estimate the equilibrium microstructure of the alloy at any time and temperature. Then the kinetics of the transformation of the austenite or gamma phase to ferrite, pearlite and/or bainite phases that tries to drive the microstructure toward an equilibrium state is governed by ordinary differential equations. The transformation of austenite or gamma phase to martensite is governed by the Koistinen–Marburger equation which is an algebraic equation (Gur and Pan 2008).

Figure 4 illustrates the result of a microstructure analysis of the experimental set up described in Sect. 2 including alpha or ferrite, pearlite, martensite and hardness distribution.

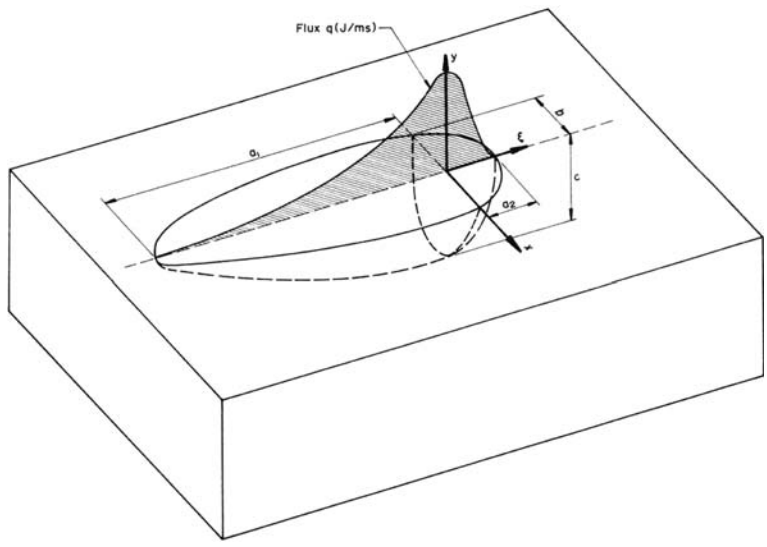

Fig. 2 Double ellipsoid model and parameters

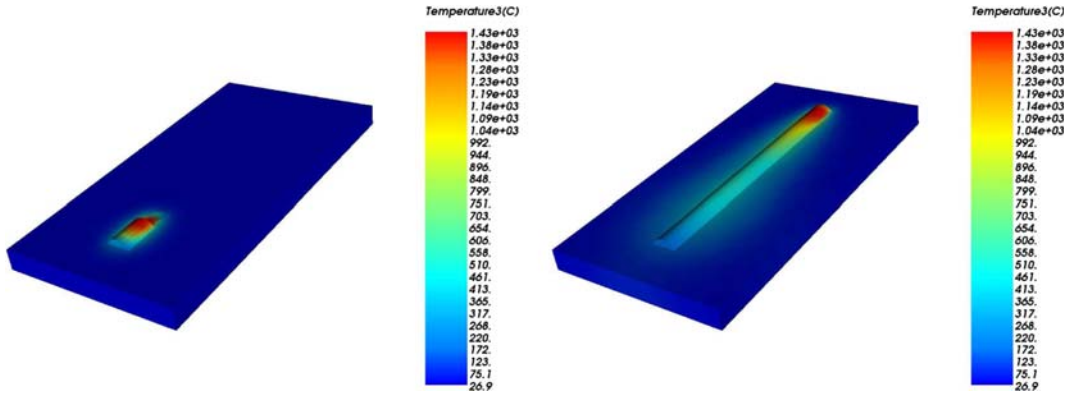

Fig. 3 Thermal results showing transient temperatures with filler metal being added after 3.5 s, *left*, and 25 s, *right*

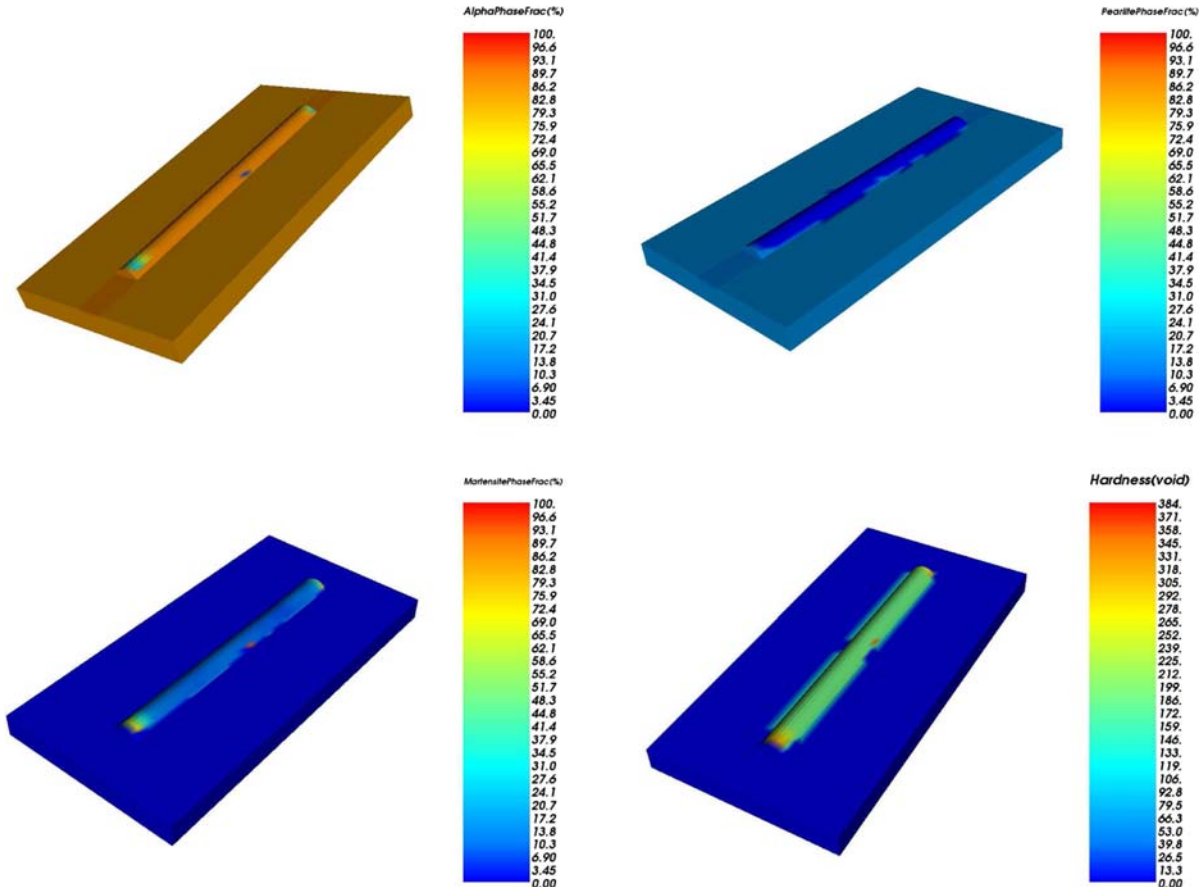

Fig. 4 Microstructure analysis of the experimental set up described in Sect. 2, alpha or ferrite phase; *top left*, pearlite phase; *top right*, martensite phase; *bottom left*, hardness distribution; *bottom right*

3.3 Stress analysis

The stress analysis uses a Lagrangian formulation to solve the conservation of momentum and mass with a thermo-visco-elasto-plastic stress-strain model based on the theory developed by Simo (1998). See Gu and Goldak (1994) and Goldak and Akhlaghi (2005) for more details on the methodology for stress analysis of welds.

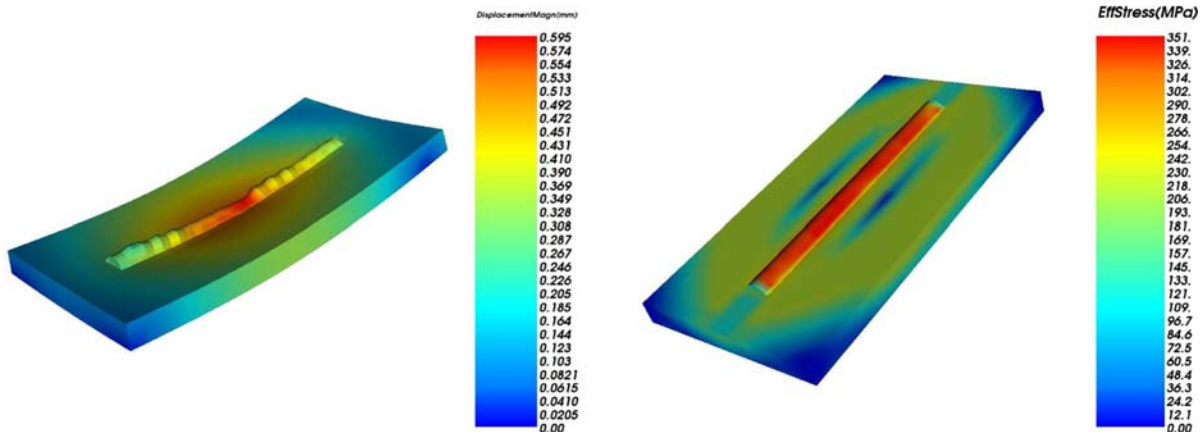

Fig. 5 Distribution of displacement (*left*) and effective or von Mises stress (*right*) in the part after welding

Figure 5 shows the displacement (left) and effective stress (right) distribution in the part. This is after welding and cool down to room temperature then the restraints have been severed at the end while the part reaches the ambient temperature.

4 Comparison

The same geometry, welding parameters and material data reported in Paradowska et al. (2005) was employed in the analysis. The material property data not provided in Paradowska et al. (2005) were taken from Anderson (1978) for a similar low-carbon steel with two changes. The first change decreased the room temperature yield stress from 375 to 250 MPa to agree with the yield stress reported in Paradowska et al. (2005). The second change was to set the compositions of the base plate and the filler metal to the compositions shown in Table 1.

The results taken from the analysis, are six components of a nodal stress that show a residual stress tensor for each FEM mesh node and interpolation gives the value at any other points in the specimen field. Therefore a full 3D field of residual stress is achievable. In order to compare with experimental data from Paradowska et al. (2005), the same path of experimental measurement described in Paradowska et al. (2005) is selected and each of the normal components of nodal stress/residual stress is plotted for comparison.

The residual stress profile for longitudinal, transverse and normal stress components measured using neutron diffraction besides computed results are shown in Fig. 6. In this figure the solid line designates computed results and the dotted line designates the experimental results. Solid red, black and light blue show the computed longitudinal, transverse and normal components respectively while dotted dark blue, pink and green lines show the experimental longitudinal, transverse and normal components.

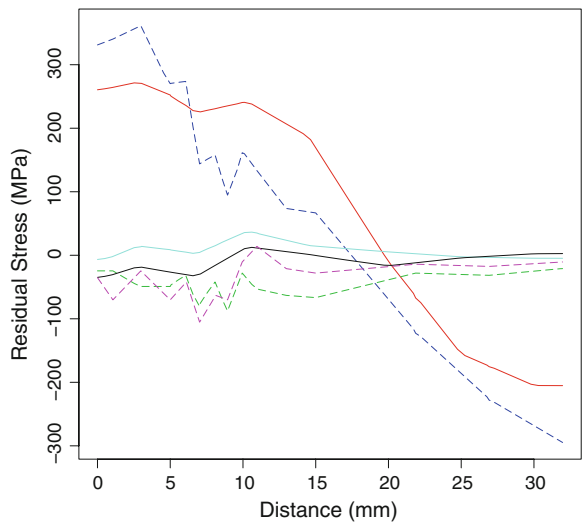

Fig. 6 This figure shows the profile of the three residual stress components measured (*dot*) and computed (*solid*) for points along the line shown in Fig. 1. In this figure the *solid line* designates computed result and the *dotted line* designates the experimental result. *Solid red, black and light blue* show the computed longitudinal, transverse and normal component respectively while *dotted dark blue, pink and green lines* show the experimental longitudinal, transverse and normal components

To quantify the deviation of computed results from experimental data, the difference as well as the statistical root mean squared error, RMSE, are determined over a set of points along the line shown in Fig. 1. One is simply the difference between the value of the computed residual stress and experimental data at each point along the line of interest. RMSE is defined as the square root of the average of the square of the differences.

The difference profile for each stress component is shown in Fig. 7. The RMSE is 79, 27 and 58 MPa for longitudinal, transverse and normal component respectively.

Since computer modeling operates on mathematical algorithm based on nominal parameter values, researchers are always trying to develop better algorithms that results in closest respond to the reality. This is endless loop though achieving the line-up match is not what researchers are following. To rigorously compare the model to experimental data, one would need replicate sets of experimental data to establish an estimate of the variability required for statistical inference.

To develop our idea of combining the regression model and FEM model for this paper by now, we conclude that the results suggest that the residual stresses for this type of weld can be predicted with useful accuracy. This accuracy for stress measurement comes from the fact argued in Gu and Goldak (1994) that seeking accuracy of stress values with errors less than $\pm 2\%$ is not realistic even if it is suggested by an analysis. In (1980) Iron and Ahmed argued that in engineering practice an accuracy of $\pm 10\%$ for stress would be considered more realistic.

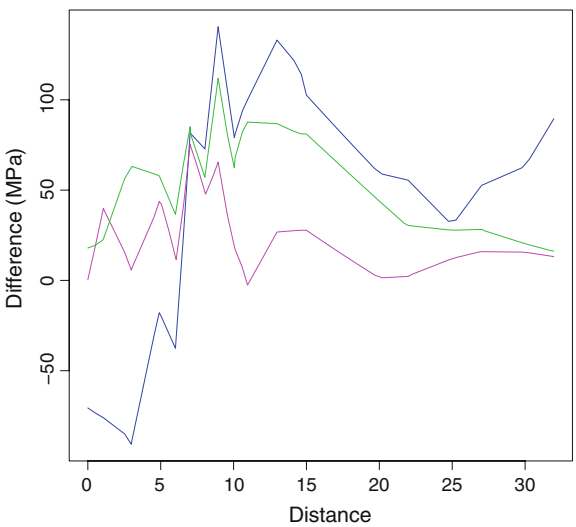

Fig. 7 The difference profile for each stress component for points along the line shown in Fig. 1. *Blue* is longitudinal, *pink* is transverse and *green* is normal component

The author's confidence in the model is based on the fact that the model uses the best available known relevant physics. This known physics is based on experiments other than welding. However the model does seem to capture the trend observed in the experiment suggesting that the model would be useful for further sensitivity analysis. Any algorithm that can predict respond better can be replaced with no effect in the idea.

5 Uncertainty analysis

A designer can reasonably employ a numerical model only if a validated predictive model is available in the design stage. In this sense, validation is the extent in which the design model and the real design agree and the extent which they differ. A designer would be delighted to have the additional capability to accommodate uncertainty in addition to a established deterministic model. Many uncertainty analysis methods try to capture this knowledge. In this paper, the Monte Carlo concept is deployed to accommodate uncertainty. Monte Carlo is a method for iteratively evaluating a deterministic model using sets of random numbers as inputs. This method is often used when the model is complex, nonlinear, or involves many parameters. A simulation can typically involve thousands of evaluations of the model, a task which may only be practical using super computers.

The conclusion in Sect. 4, suggests that the model can be employed for a sensitivity analysis in order to provide some information on uncertainty.

The first and simple step in an uncertainty analysis using Monte Carlo is to select a parameter with an assumed distribution and measure the response of the system. To run such a test, the current of the weld arc in the welding procedure is taken as one of the uncertain parameters reported in papers and practice.

The value used for current is 280 amperes (Anderson 1978). Reference Pan (2003) monitored experimentally the variation of welding arc while welding different sets of experiments and these plots

provide an estimate of current distribution while welding. Under the assumption of a normal distribution, a normal distribution with mean $\mu = 280$ amperes and standard deviation $\sigma = 5$ is assumed for an uncertainty analysis. These values were obtained from the sample mean and standard deviation from data in Pan (2003).

A sample of size 30 was taken for this distribution so that approximate normality holds by the Central Limit Theorem. Each test takes 13 min on a desktop computer and using four CPUs in parallel the analysis CPU time is 1 h and 40 min.

Solving a full analysis described in Sect. 3 provides thermal, micro-structure and stress analysis result for the plate in Sect. 2. So far we have been working on the line of interest in Fig. 1 which is the line of experimental measurement. Therefore we continue working on this line to develop the idea however this algorithm can be used for any point, line, area or volume in the whole field or plate.

Regarding our sample size of 30, we get 30 different results for each sample. In other words, we run 30 tests with 30 different values for current taken from a normal distribution with $\mu = 280$ and $\sigma = 5$. Therefore for each FEM mesh point in the plate we have 30 different values of results such as residual stress such that we can compute mean and standard deviation for each point. In fact, we have generated the distribution for each point of the plate. Each point has its own distribution's characteristic (μ, σ) that shows the variation in results due to variation in a parameter like current.

Back to the line of interest in Fig. 1 which is the line of experimental measurement. This line has 78 points in our FEM mesh and every point has its own μ and σ. Figure 8 shows the μ and $\pm 3\sigma$ for each point along the line of interest. This kind of plot shows the result of how uncertainty of a parameter like current distribution affects a result like the residual stress. It also shows which locations on the specimen are more sensitive. Red, green and blue lines illustrate higher bound, $+3\sigma$, mean, μ, and lower bound, -3σ respectively in this figure.

This approach is certainly limited by the computation time and resources such that it is not practical for a large number of parameters. Regarding numerical modeling of a weld, there are a great number of parameters in the modeling. For instance more than 300 parameters for the model used to analyze the

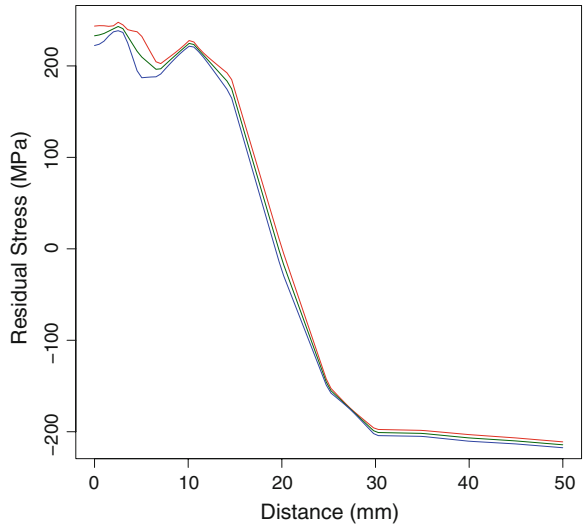

Fig. 8 Uncertainty distribution for longidutional component of residual stress for points along the line shown in Fig. 1

weld have effect on the results. Mathematical algorithms employed in computational modeling, include parameters whose values are not known precisely but may vary within some ranges that reflect our incomplete knowledge or uncertainty regarding them. Generally speaking the objective of uncertainty or sensitivity analysis is to quantify the effects of parameter variations on computed results.

In this paper an alternative way employed to accommodate uncertainty is point-by-point regression in the case of studying many parameters particularly interrelated parameters is presented. The idea comes from multidimensional least square regression analysis in which a hyper-plane is fitted to the points positioned in the multidimensional space of our parameters. We call it point-by-point because each numerical point of our specimen has its own hyper-plane to estimate the response for that point. The algorithm is explained in an analysis carried out on four double-ellipsoid parameters of weld arc defined in Goldak and Akhlaghi (2005) including a_1, a_2, b and c which are the tail, front, width and depth axes lengths respectively.

5.1 Experimental design

A full factorial experimental design is employed to keep the highest resolution such that four parameters and three levels due to second order fitting results in

Table 2 Design matrix, $X_{81\times15}$

Run no.	Constant	a_2	a_1	b	c	a_2a_1	a_2b	a_2c	a_1b	a_1c	bc	a_2^2	a_1^2	b^2	c^2
1	1	6	13	6	4	78	36	24	78	52	24	36	169	36	16
2	1	7	13	6	4	91	42	28	78	52	24	49	169	36	16
3	1	8	13	6	4	104	48	32	78	52	24	64	169	36	16
.	.	.	.	.	.	.	.	.	.	.	.	.	.	.	.
.	.	.	.	.	.	.	.	.	.	.	.	.	.	.	.
.	.	.	.	.	.	.	.	.	.	.	.	.	.	.	.
81	1	8	15	8	6	120	64	48	120	90	48	64	225	64	36

Table 3 Values assigned to parameters in mm

Parameter	High (mm)	Mid (mm)	Low (mm)
a_1	15	14	13
a_2	8	7	6
b	8	7	6
c	6	5	4

$3^4 = 81$ different settings. Therefore the design matrix, X, for the main effects is 81 by 5 including *intercept*, a_1, a_2, b and c for 5 columns by 81 different setting in each row. Adding 2-way interactions and second order of effects increases the number of column to 15; 1, a_1, a_2, b, c, a_1a_2, a_1b, a_1c, a_2b, a_2c, bc, a_1^2, a_2^2, b^2, c^2 such that a final design matrix, X, is 81 by 15 (Table 2). Two-way interactions can be seen as the area formed by two lengths considering we can have the same area with different lengths.

To accommodate the levels of factors in double ellipsoid parameters, ±1 mm variation from the default setting is given to each parameter. This range is conservatively and intuitively taken so that it involves even rare possible variations. The levels were selected to cover a reasonable range of weld sizes however any number of levels an interval spacing could be utilized. Table 3 shows the high, mid and low values assigned.

5.2 Selection of response

We employed the multi-project mode of VrWeld software to run the whole pattern of experiments using four CPUs in parallel. Each single project takes 13 min and the whole set of 81 experiments is computed in 4 h and 40 min including thermal, micro-structure and stress analysis on a desktop quad core machine. Regarding experimental data available, this analysis is directed to residual stress for the nodes along the line of experimental measurement in Fig. 1 at the final time step. Note that the method is not limited to these specific responses, nodes or time steps.

Look at the problem from each FEM mesh node in the field or plate, each node has a set of 81 values computed from every combination of parameters that is one row in design matrix X, Table 2. Hence we can write them in a column matrix form of responses $Y_{81\times j}$ where j is from 1 to the total number of nodes. Back to the line of interest or experimental measurement, the total number of nodes along this line is 78 and therefore j varies from 1 to 78 in our case. In other words, our response matrix is $Y_{81\times78}$. It is shown in Table 4.

5.3 Regression model

The regression model 1 is solved by least-squares which has a closed form solution given by Eq. 2 where X and Y are the design and response matrix respectively.

$$Y = X\beta + \epsilon \tag{1}$$

$$\widehat{\beta} = (X^TX)^{-1}X^TY \tag{2}$$

In our case, $Y_{81\times78}$ is a response matrix created in step 2 (Table 2) and $X_{81\times15}$ is a response matrix created in step 1 (Table 4). Therefore β should be 15×78 for matrix multiply compatibility (Table 5).

The dimensions show the number of terms in the design matrix (number of columns in Table 2) and number of nodes selected (number of columns in Table 4) respectively. It means that we have specific coefficients for every node that forms a function to

Table 4 Response matrix scheme $Y_{81\times78}$

	$node_1$	$node_2$	$node_3$	.	.	.	$node_{78}$
run_1	$Y_{1\ 1}$	$Y_{1\ 2}$	$Y_{1\ 3}$	.	.	.	$Y_{1\ 78}$
run_2	$Y_{2\ 1}$	$Y_{2\ 2}$	$Y_{2\ 3}$	.	.	.	$Y_{2\ 78}$
run_3	$Y_{3\ 1}$	$Y_{3\ 2}$	$Y_{3\ 3}$	.	.	.	$Y_{3\ 78}$
.	.	.	.	.	.	.	.
.	.	.	.	.	.	.	.
.	.	.	.	.	.	.	.
run_{81}	$Y_{81\ 1}$	$Y_{81\ 2}$	$Y_{81\ 3}$	.	.	.	$Y_{81\ 78}$

Table 5 Coefficient matrix scheme $\widehat{\beta}_{15\times78}$

	$node_1$	$node_2$	$node_3$	.	.	.	$node_{78}$
1	$\beta_{0\ 1}$	$\beta_{0\ 2}$	$\beta_{0\ 3}$	.	.	.	$\beta_{0\ 78}$
a_2	$\beta_{1\ 1}$	$\beta_{1\ 2}$	$\beta_{1\ 3}$	.	.	.	$\beta_{1\ 78}$
a_1	$\beta_{2\ 1}$	$\beta_{2\ 2}$	$\beta_{2\ 3}$	.	.	.	$\beta_{2\ 78}$
b	$\beta_{3\ 1}$	$\beta_{3\ 2}$	$\beta_{3\ 3}$	.	.	.	$\beta_{3\ 78}$
c	$\beta_{4\ 1}$	$\beta_{4\ 2}$	$\beta_{4\ 3}$	.	.	.	$\beta_{4\ 78}$
a_2a_1	.	.	.	.	.	.	.
a_2b	.	.	.	.	.	.	.
a_2c	.	.	.	.	.	.	.
a_1b	.	.	.	.	.	.	.
a_1b	.	.	.	.	.	.	.
bc	.	.	.	.	.	.	.
a_2^2	.	.	.	.	.	.	.
a_1^2	.	.	.	.	.	.	.
b^2	.	.	.	.	.	.	.
c^2	$\beta_{14\ 1}$	$\beta_{14\ 2}$	$\beta_{14\ 3}$	.	.	.	$\beta_{14\ 78}$

compute the residual stress for the node from a set of given a_2, a_1, b and c parameters.

5.4 Working with the model

The least-square regression model can be written in matrix form for regression responses $\widehat{Y}$ when we have computed coefficient matrix, $\widehat{\beta}$ (Table 5) by Eq. 3;

$$\widehat{Y} = X\widehat{\beta} \tag{3}$$

In our case, the result has the form of Eq. 4;

$$\widehat{Y}_{1\times78} = X_{1\times15}\widehat{\beta}_{15\times78} \tag{4}$$

where the $\widehat{\beta}$ shown in the Table 5 is computed from Eq. 2. How the regression Eq. 4 works is summarized below.

(a) Select a value of interest for the parameters a_1, a_2, b, c in the range of Table 3.

(b) Form X which is a row matrix of [1, a_1, a_2, b, c, a_1a_2, a_1b, a_1c, a_2b, a_2c, bc, a_1^2, a_2^2, b^2, c^2].

(c) Use Eq. 4 to compute response, $\widehat{Y}$.

(d) Interpretation is the value of residual stress for each node along the line of interest in Fig. 1 using the regression model.

To compare the residual stress computed from the regression model with the residual stress computed from FEM analysis, we select an arbitrary combination of $a_1 = 15$, $a_2 = 6$, $b = 7$, $c = 4$. Figure 9 shows how well this regression model can emulate an FEM prediction.

It is easily understandable now that the dimension of Y can be increased to all the nodes in the analysis, e.g., 5,724 for problem analyzed in this paper to cover the whole field. Consequently, $\widehat{Y}$ also has the dimension of the complete set of nodes and covers the whole field. The response is not also limited to the residual stress. Any output from the FEM model can

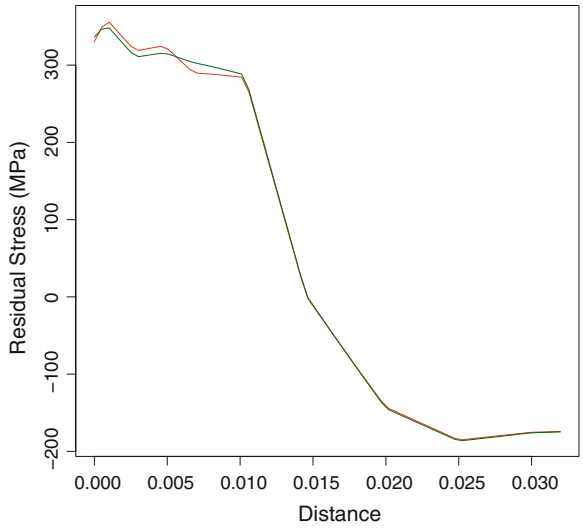

Fig. 9 Comparing FEM and regression model prediction for longidutional component of residual stress along the line shown in Fig. 1. *Red line* is FEM prediction and *green line* shows regression

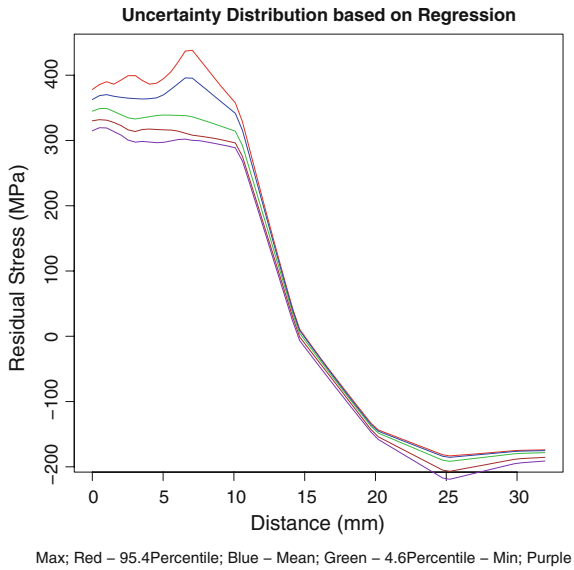

Fig. 10 Uncertainty distribution using regression model based on variation of double ellipsoid parameters

be considered as a response. This means that the algorithm works for any result at any point at any time of the analysis.

6 Perturbation analysis

Equation 3 is a continuos well conditioned mathematical equation. The computing time depends on the dimension of matrices. Therefore it is well suited for perturbation analysis such as Monte Carlo with an acceptable numbers of runs.

A normal distribution is employed for the four double ellipsoid parameters as it is commonly used. This seems a reasonable assumption. However based on the application and analysis of probability of occurrence other distributions could be used.

Ten-thousand random values are generated for each of the double ellipsoid parameters and the residual stress is computed along the line of interest using the regression estimator $\widehat{Y}$. Figure 10 illustrates the uncertainty distribution using the regression estimator based on a normal variation of the double ellipsoid parameters. In this figure, the mean value is plotted in green showing the average residual stress and the maximum and the minimum bound is plotted in red and purple respectively. The blue line represents the 95.4% and brown the 4.6%.

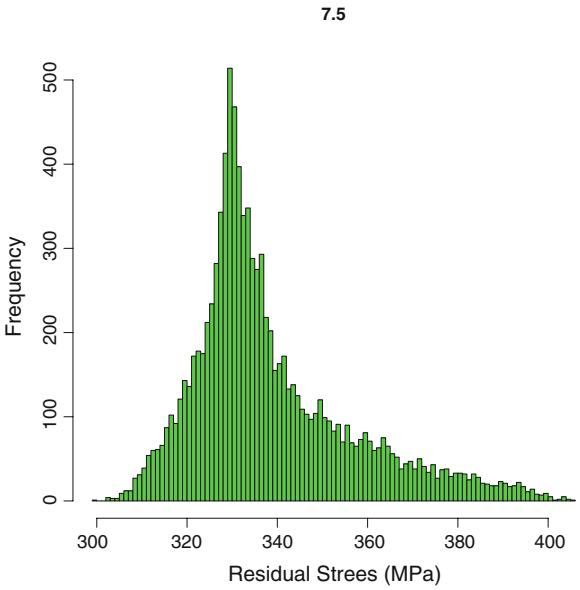

Fig. 11 Distribution of residual stress for the node distanced 7.5 mm from the mid-weld

In fact, this plot is extracted from a histogram of 78 nodes along the line of interest showing the distribution of residual stress. As a sample Fig. 11 shows this distribution for the node 7.5 mm from the weld center line. A check of Fig. 10 shows that this point is the point that has a significant variation from the mean. The histogram in Fig. 11 shows that for a

normally distributed parameters, there is a very rare chance of getting a residual stress 400 MPa, about 70 MPa more than expected value. Considering 95 and 99% percentiles for this histogram are (315,378) and (308,396) MPa respectively.

7 Conclusion

Numerical algorithms are well developed now to predict the behavior of many systems. However recent models can require a large number of parameters to approximate the behavior. Usually these parameters are taken as fixed values within the algorithm extracted from a constant entry, table, function and so on. In fact no parameter is fixed as assumed and inherent variation effects the solution. Although many effective stochastic algorithms offer a methodology to accommodate the uncertainty in parameters, they are limited by the computational power available to a certain usually small number of parameters.

From statistics, regression models are well enough understood to provide a good estimate of the system based on the response of the system. However these models can be valid for only a specific range of each parameter and this range is usually small particularly when the number of parameters is large. The idea of breaking the whole range of parameters into a combination of pieces with small range and extracting different regression model for each one, can be a good mathematical solution but it is limited by the cost and time of running a different test for each range and extracting its specific model.

Combining regression modeling and numerical modeling may develop a sophisticated solution to reduce the limitations of both sides. The idea is simple. Employ numerical modeling such as FEM to provide a nodal response field. Then create a node-by-node regression model from FEM analysis to cover the whole field. Briefly create and use a regression model to predict uncertainty due to the combination of variation in a large number of parameters. It is also possible to evaluate the combination of parameters in the space of parameters to determine the closest model to the observed reality. This argument is true if two prerequisites are satisfied. First the numerical model can capture the behavior of the interest in an acceptable band compared to the experimental data. Secondly the pieces of range selected for the regression model satisfies the statistical confidence level (adaptive refinement might be needed).

A welding test problem with experimental data from Paradowska et al. (2005) was used. Residual stress was computed and the results were compared with experimental data using the difference and root mean squared error, RMSE, to show that the numerical prediction captures the behavior of residual stress. Point-by-point least square fitting was used for regression. This regression model was compared to the numerical result to show consistency. Uncertainty analysis based on a Monte Carlo analysis was performed to provide uncertainty distribution. The CPU time for four parameters using a regression model with 10,000 random value was less than a second.

References

Anderson, B.A.B.: Thermal stresses in a submerged-arc-welded joint considering phase transformation. Trans. ASME J. Eng. Mater. Technol. **100**, 356–362 (1978)

Goldak, J., Akhlaghi, M.: Computational Welding Mechanics, Springer, ISBN 0-387-23287-7 (2005)

Goldak, J.A., Chakravarti, A., Bibby, M.J.: A new finite element model for welding heat sources. Trans. AIME **15B**, 299–305 (1984)

Gu, M., Goldak, J.: Steady state formulation for stress and distortion of welds. J. Eng. Ind. **116**, 467–474 (1994)

Gur, C.H., Pan, J.: Hand Book of Thermal Process Modelling of Steels. CRC Press, London (2008)

Henwood C., Bibby M.J., Goldak J.A., Watt D.F.: Coupled transient heat transfer—microstructure weld computations (Part B). Acta Met. **36**(11), 3037–3046 (1988)

Iron, B.F., Ahmad, S.: Techniques of Finite Elements, Ellis-Horwood Limited. ISBN 0-85312-130-3 (1980)

Kirkaldy, J., Venugoplan, D.: Prediction of micro-structure and hardenability in low alloy steels, phase transformation in ferrous alloys. In: Proceedings of International Conference, 4–6 Oct 1983

Kumar, R., Coulombe, M., Tchernov, S., Goldak, J.A., Johnson, E., El-Zein, M.: A model equation for the convection coefficient for thermal analysis of welding structures. In: 8th International Trends in Welding Research, Callaway Gardens Resort, Pine Mountain, Georgia, USA, 2–5 June 2008

Pan, J.: Arc Welding Control. Book published by Woodhead Publishing, ISBN 185573687X (2003)

Paradowska, A., Price, J.W.H., Ibrahim, R., Finlayson, T.: A neutron diffraction study of residual stress due to welding. J. Mater. Process. **164–165**, 1099–1105 (2005)

Simo, J.C.: Numerical analysis of classical plasticity. In: Ciarlet, P.G., lions, J.J. (eds.) Handbook for Numerical Analysis, vol. IV. Elsevier, Amsterdam (1988)

Watt, D.F., Coon, L., Bibby, M.J., Goldak, J.A., Henwood, C.: Modelling microstructural development in weld heat-affected zones (Part A). Acta Met. **36**(11), 3029–3035 (1988)